Astron. Astrophys. 320, 405–414 (1997)

ASTRONOMY
AND
ASTROPHYSICS

[O III] λ 5007 wing variations and changes of Fe II optical multiplets in NGC 5548⋆

S.G. Sergeev, V.I. Pronik, Yu.F. Malkov, and K.K. Chuvaev⋆⋆

Crimean Astrophysical Observatory, P/O Nauchny, 334413 Crimea, Ukraine

Received 4 October 1995 / Accepted 5 August 1996

Abstract. The variations of the [O III] λ 5007 line profile in NGC 5548 are examined from CCD spectra obtained at the Ohio State University and Crimean Astrophysical Observatory in December 1988 – October 1994. We have found the total flux of [O III] λ 5007 line to be variable, so the spectral calibration based on the assumption of non-variability of [O III] λ 5007 line is not absolutely correct. The variations are much more pronounced in the far wings of the line profile ($\sim$ 1100 km s^{-1}). Assuming the central part of the line profile is non-variable, we analyzed the variations of the red and blue wings relative to the profile center. We have found that these variations can be explained in terms of a reaction to the ionizing radiation changes with a transfer function spreading up to several hundred days. Perhaps, the "real" constant flux is localized in the narrow [O III] line which belongs to the NLR and has a transfer function of about several hundred years, while the broad wings are emitted from the outer BLR. These wings may belong to Fe II λ 5018 and/or [O III] λ 5007. The transfer function of the blue wing is narrower, with a peak shifted to the zero lag by ∼200 days relative to the transfer function of the red wing. Both wings, and especially the blue wing, show weak reaction near the zero lag. These facts must exclude both pure radial and round motion, but may suggest a lack of emitting gas near the line of sight and the presence of an outflow component. The Fe II λ 5169 line shows similar behavior to the [O III] λ 5007 wings. It confirms Fe II λ 5018 is the main contributor to the [O III] wings or that the broad [O III] is emitted at the same distance from the central engine as the Fe II. The assumption about the presence of "short" and "long" lag spectral components, one of which varies similarly to the Hβ line and the other similarly to the [O III] λ 5007 wings, permits us to separate these components. The decomposition of the spectra shows that all observed Fe II multiplets have a high lag value of the order of several hundred days, pointing to the typical size of the region which emits these lines. The decomposition also shows that there is a short lag component in the red wing of [O III] λ 5007 line. According to the centroid of this line (≈ 5032 Å) it may be identified with the Si II λ 5041, 5056 or He I λ 5016, 5048.

Key words: galaxies: active – galaxies: individual: NGC 5548 – galaxies: Seyfert – lines: profiles

1. Introduction

The Seyfert 1 galaxy NGC 5548 was an object of the high-rate monitoring for the five years (Peterson et al. 1991; Peterson et al. 1992; Peterson et al. 1994; Korista et al. 1995). A large amount of the spectral data obtained through this monitoring makes possible the study of the broad line variations and their reaction to the continuum changes, assuming the photoionized BLR (broad-line region) gas responds to the variations of the continuum source. The light-travel time effect will delay and smooth the line response by a way which depends on the size and geometry of a given line emission region.

An interesting spectral feature which we will investigate here are the broad wings of the [O III] λ 5007 line. These wings are visible not only in the NGC 5548 spectrum, but are also pronounced and even much larger in Akn 120, NGC 7469 etc. (van Groningen & de Bruyn 1989). One interesting question is whether this spectral feature varies and, if so, how much are its changes delayed with respect to the continuum variations. Following the echo-mapping scheme (Blandford & McKee 1982) we will try to recover the transfer function to make some conclusions about the size and geometry of the region emitting the broad wings of [O III] λ 5007. We will also study the variations of Fe II λ 5169 in order to compare its behavior with the behavior of the [O III] λ 5007 wings. We will also examine the reliability of the assumption that the [O III] λ 5007 line is non-variable, since most spectra are calibrated using this line. It concerns not only the NGC 5548 nucleus, but also other active galactic nuclei.

From another viewpoint it is interesting to know what these wings are. To explain the red shelf seen in many Hβ profiles, Osterbrock and Shuder (1982) attributed this shelf to

Send offprint requests to: S.G. Sergeev

⋆ Table 2 is only available in electronic form at the CDS via anonymous ftp 130.79.128.5

⋆⋆ Deceased, 15 November 1994

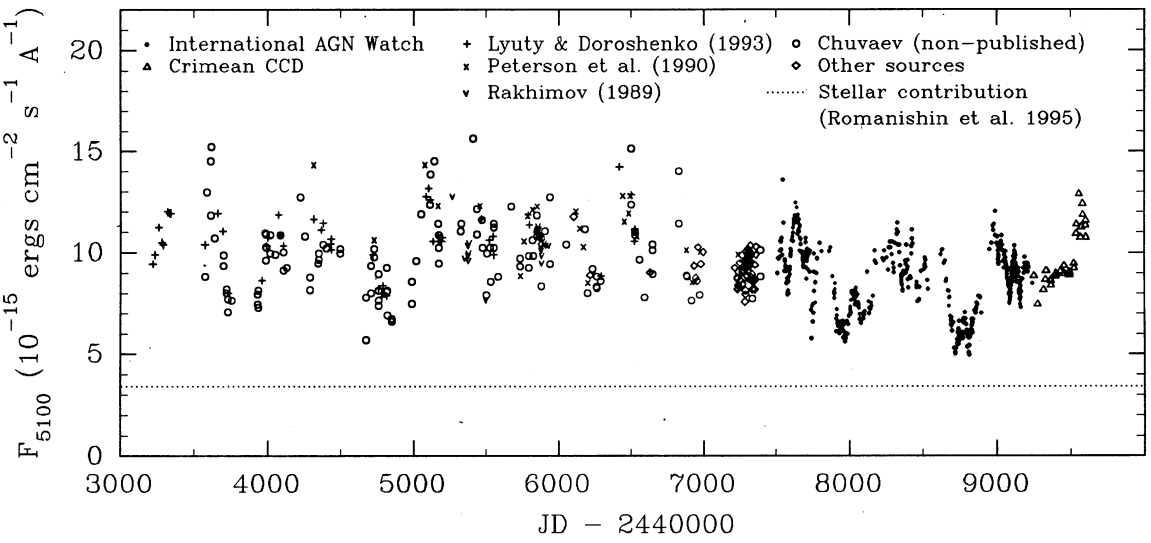

Fig. 1. Optical continuum of NGC 5548 nucleus at λ5100Å based on the International AGN Watch results and other source data.

Fe II λ 4924, 5018 emission. In this case the broad [O III] λ 5007 wings may be the Fe II λ 5018 line. The optical Fe II multiplets were first identified in 3C 273 by Wampler & Oke (1967) (see also Phillips 1978). The possibility that there is a broad [O III] λ 4959, 5007 emission has also been discussed (Crenshaw & Peterson 1986; van Groningen & de Bruyn 1989; Stirpe, van Groningen & de Bruyn 1989). In addition, there is a suspicion that the weak broad emission near 5050 Å is present (Crenshaw & Peterson 1986). This emission may be identified with the Si II λ 5041, 5056 lines (van Groningen 1984). The difficulty with line identification is due to the lines of interest being broad, weak and blended with other broad and narrow lines. Thus we have a problem of spectral decomposition to remove some features and to study others. De Robertis (1985) gives a procedure to remove the red shelf from the Hβ profile assuming the shelf is entirely Fe II emission. Other methods which include [O III] λ 4959, 5007 as the contributors in addition to Fe II lines were proposed by Meyers & Peterson (1985) and Crenshaw & Peterson (1986), and were based on the fit of the observed profile (of Akn 120, NGC 5548 etc.) using some assumptions. We will decompose the observed spectrum of NGC 5548 following the method based not on the fit of a single spectrum, but on the variability characteristics of all our spectra.

2. Observations

During the international program of NGC 5548 monitoring, a large amount of spectral data was obtained (Peterson et al. 1991; Peterson et al. 1992; Peterson et al. 1994; Korista et al. 1995). In the present paper we have used the Ohio State University (OSU) CCD spectra where the monitoring was carried out on the 1.8-m Perkins Telescope (JD 2447517–2448898) and the Crimean Astrophysical Observatory CCD spectra (2.6-m Shajn Telescope, JD 2448630–2449601). The entrance aperture of the first (most homogeneous) data set was $5''.0\times 7''.5$. For the second data set the aperture has been changed from $2''.3\times 11''$ to $3''.0\times 11''$ (so these data are slightly inhomogeneous). The spectral resolution for both data sets was 9Å. Preliminary analysis had shown the width of transfer function may spread up to hundreds of days. This implies that the continuum must be known for several years before JD 2447517. Meantime, the high-rate optical monitoring of NGC 5548 (Peterson et al. 1991; Peterson et al. 1992; Peterson et al. 1994; Korista et al. 1995) where the continuum at 5100 Å was measured begins only from JD 2447509. To fill the missing span we added earlier data from other sources. This consisted of photometric data: the U-band measurements (Lyuty & Doroshenko 1993), the V-band measurements (Rakhimov 1989); and spectral data: Chuvaev (1987), Chuvaev non-published data, Stirpe, de Bruyn & van Groningen (1988) ([O III] equivalent widths), Stirpe & de Bruyn (1991), Peterson et al. (1990), Peterson, Korista & Cota (1987), Netzer et al. (1990) (continuum at 5100Å or nearby) and non-published data obtained in the Crimean Observatory (continuum near the Hα line). The intercalibration of these heterogeneous data is a difficult problem. We have used all information which we knew about the instrumental setting of these data sets. The detailed justification of the intercalibration procedure is given in Appendix A. The entire light curve of the continuum at 5100Å, beginning in 1977, is shown in Fig. 1.

The "pre-AGN Watch" calibrated data which we assembled have been obtained with different instruments, and have been differently reduced and analyzed. In several cases the continuum flux was not measured at 5100Å. Thus these intercalibrated data in Fig. 1 seem to be erroneous. Here we will not discuss the value of the errors for each data set as well as intercalibration errors, because it is not easy to estimate all the sources of uncertainty, and there is no "standard" data set in order to evaluate the errors (as was done in AGN Watch campaign paper series on NGC 5548). Moreover, the entire continuum light curve of NGC 5548 and its analysis is not a target of this work. However, we believe that it is useful to publish the calibrated pre-AGN

Table 1. Codes for "pre-AGN Watch" data origin

Id.	Reference	Instrument	Wavelength range
1	Present work (Crimean data) and Chuvaev (1987)	2.6-m + Image tube	[O III] λ 5007 equivalent width
2	Netzer et al. (1990)	1.0-m + CCD	4710–4760Å, 5375–5575Å
3	Peterson et al. (1987,1990)	1.8-m + IDS	≈5000Å
4	Stirpe et al. (1988)	2.5-m + IPCS	[O III] λ 5007 equivalent width
5	Stirpe & de Bruyn (1991)	2.5-m + IPCS	≈5100Å
6	Present work (Crimean data)	2.6-m + CCD	≈6330Å
7	Lyuty & Doroshenko (1993)	0.6-m	U-band photoelectric photometry
8	Rakhimov (1989)	0.7-m	V-band photoelectric photometry

Watch data, which we show in Table 2. The codes of data origin are given in Table 1.

3. Variability analysis

3.1. The method of determination of the transfer function

The reverberation-mapping ideas have been developed by Blandford & McKee (1982). Under some basic assumptions (Peterson 1994), the emission-line flux as a function of time is generally assumed to be described by the equation

$$L(t) = \int_0^\infty C(t-\tau)\Psi(\tau)d\tau. \quad (1)$$

where $C(t)$ is the continuum light curve, $L(t)$ is the emission-line light curve, and $\Psi(t)$ is the transfer function. To find the transfer function it is necessary to invert the integral equation (1). Unfortunately, inverting convolution equations is known as notoriously difficult and ill-posed task. However, the problem of the inversion can be simplified if the kernel $\Psi(t)$ is *parameterized*, thus we can attribute the transfer function to a given class of functions defined by a fixed number of numerical parameters. Such a *limited* task allows us to solve convolution equation without inverting it really. We have only to vary the numerical parameters to find the minimum of

$$\Phi = \sum_t (L(t) - \int_0^\infty C(t-\tau)\Psi(\tau)d\tau)^2. \quad (2)$$

Any reasonable multi-dimensional optimization method may be used for this purpose.

To parameterize the transfer function, we have selected several nodes on the time axis. The linear interpolation of the transfer function between nodes was assumed. We set the response for the negative lag and the response beyond the last node to zero. So, we have presented the transfer function as a family of straight lines which connect the individual points. While the positions of the nodes were fixed, their values are those parameters which represent and uniquely define any virtual solution in terms of this limited task. Then we have to find the transfer function by optimization of the node values with the target function equal to RMSD (root-mean-square deviation) between the continuum light curve convolved with the transfer function and the line light curve (Eq. 2). The enhanced Newton's method for multi-dimensional optimization was used. This algorithm requires only the starting values of the parameters. In practice, we started optimization with several arbitrary realizations of the transfer function to check whether there is a single solution.

Some arbitrariness is present only in the number of the nodes (the lower numbers will give the simpler cases, beginning with the triangle-shape transfer function) and their time spacing. The number of nodes, however, can be reasonably adjusted empirically. If there are too many nodes, the solution will be undefined – the same RMSD will correspond to widely different solutions. As concerns the node positions, we can start with equidistantly spaced points, then to add nodes at the places where a steep gradient suspected and to remove the nodes which seem to be non-informative.

To check the reliability of the calculated transfer function we performed a Monte-Carlo simulation. The basic fit for the line light curve was affected by the Gaussian noise with the standard deviation equal to RMSD of observed values from this fit. Thus we assumed that all measurements have equal weights and the degree of freedom approximately equals the number of points. Such a test, repeated many times, provides us with information concerning what deviations from the most probable solution can be expected.

3.2. Changes in the [O III] λ 5007 absolute flux

The absolute flux of [O III] λ 5007 line was measured during the NGC 5548 international monitoring campaign. The [O III] line light curve based on these results (Peterson et al. 1991; Peterson et al. 1992; Peterson et al. 1994; Korista et al. 1995) is shown in Fig. 2a. For further analysis, we have excluded only one measurement marked by an open circle (Fig. 2a). No significant variations were detected, but there is a systematic flux decrease by about 5%, and a wide minimum on JD≈ 2448200. Despite the fact that these features are comparable with the observational errors, we can still address the question of whether the suspected variations can be explained as a response of [O III] line to the ionizing radiation changes. As a first step we have

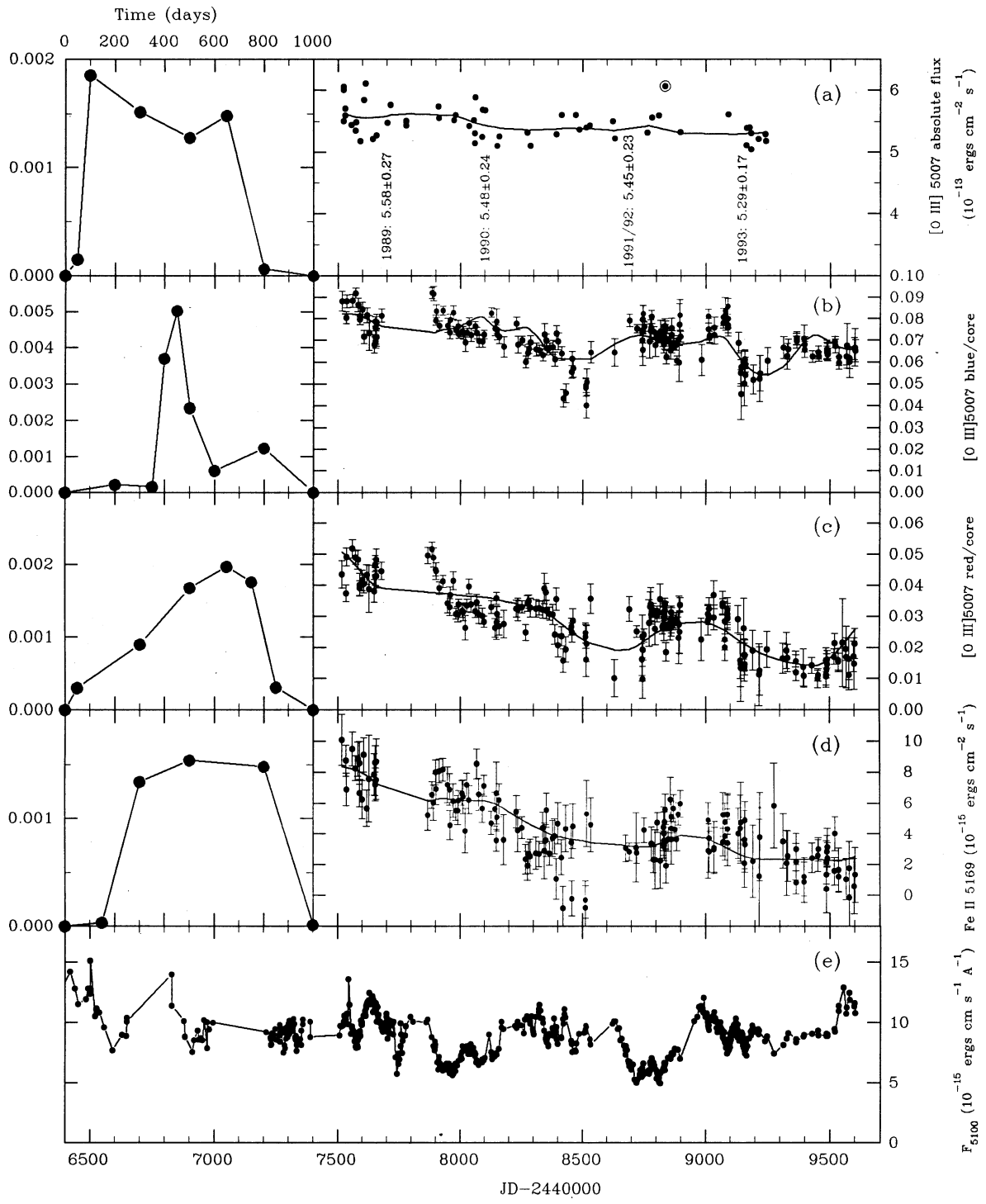

Fig. 2. a The [O III] λ 5007 line light curve obtained by the International AGN Watch of NGC 5548 is shown in the right panel. The encircled point has been rejected. The solid line is the best fit obtained with the transfer function shown in the left panel. Unfortunately, the reliability of this solution is very poor due to small amplitude of variations of [O III] line flux, but it can still be concluded that the transfer function spreads up to hundreds of days in time. **b,c** [O III] λ 5007 wing variations in NGC 5548. The right panels show the red/blue wing to core ratios. The solid lines are the best fits obtained with the transfer functions shown in the left panels. **d** Fe II λ 5169 line variations and the best fit by the transfer function shown in the left panel. **e** The continuum light curve at 5100Å (rest frame) used to recover the transfer functions.

tried to find a flat-top transfer function using the continuum light curve shown in Fig. 1. We found the best solution when the reaction began with a 50 day lag and finished with a 570 day lag. Then we selected several nodes on the time axis and found the transfer function according to the method described in Sect. 3.1. The result is presented in the left panel of Fig. 2a.

The Monte-Carlo simulation shows that the obtained solution is very poorly determined, because the observational errors are comparable with the variation amplitude. Nevertheless, we can conclude that it is possible to explain the above mentioned features of the [O III] line light curve by the response to the ionizing radiation changes with the transfer function with typical lag of the order of several hundred days.

We have done the extrapolation of the variations of [O III] back to 1977 using Eq. 1 with continuum light curve $C(t)$ shown in Fig. 1. According to the obtained transfer function (Fig. 2a, left panel), the [O III] λ 5007 line flux must have varied by about 15% since 1977. It implies that the measurements of continuum based on the assumption that the [O III] λ 5007 line is non-variable will give us the same error. Strictly speaking, we must correct the continuum measurements in Fig. 1 for the [O III] variability, then repeating the deconvolution process. However, the continuum variations have much larger amplitude than the [O III] ones, therefore such a correction will not be significant.

The next question we can address is that of the variable component in the [O III] λ 5007 line. It seems realistic that only some unknown broad species near [O III] λ 5007 can vary, while the narrow forbidden line cannot be variable on the time scale of several hundred days. We have subtracted from the continuum light curve the stellar contribution of $3.4 \cdot 10^{-15}$ergs cm^{-2} s^{-1} Å^{-1} (Romanishin et al. 1995) to obtain the variable continuum. Convolving this continuum with the transfer function (Fig. 2a, left panel) we have obtained the light curve of the variable part of [O III] flux. Subtracting this light curve from the total [O III] light curve (Fig. 2a, right panel), we have estimated the flux of the [O III] constant component as $3.9 \cdot 10^{-13}$ergs cm^{-2} s^{-1}, i.e. the variable component is about 40% of the constant component. Despite the large uncertainties in the determination of the last value, it can be suggested that [O III] λ 5007 constant flux dominates. It is also evident from the fact that the NLR (narrow-line region) has a size of order one hundred light years for the objects with spatially resolved [O III]-emitting region (e.g. NGC 4151), in contrast to the width of the transfer function of hundreds of days which we have found. Thus we must attribute the variable part of the [O III] λ 5007 line to the outer BLR rather than to the NLR. Let us suppose that the variable component is a broad line which may be [O III] λ 5007 or not. If so, we can expect a large variability amplitude in the far wings of the [O III] λ 5007 line profile.

3.3. Changes in [O III] λ 5007 wings

Assuming that the [O III] λ 5007 line profile consists of a non-variable narrow component and a variable broad component, we must expect the central part of the line to be the most stable, while the far wings are the most variable. In this case the wing to core flux ratio will be a good characteristic of wing variations. Since this ratio reflects the profile shape, no spectrum scaling procedure is required. However, the approximate scaling will be necessary to homogenize the OSU and Crimean measurements as described below. For this purpose, we used the standard calibration (Peterson et al. 1991; Peterson et al. 1992; Peterson et al. 1994; Korista et al. 1995) based on the *total* flux of the [O III] λ 5007 line.

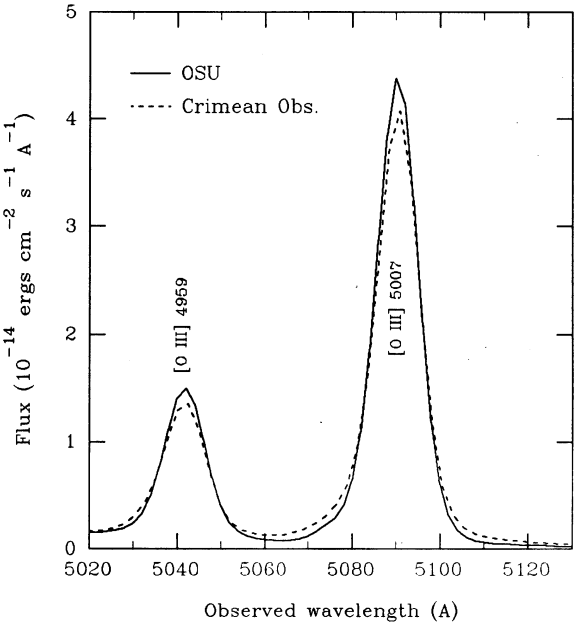

Fig. 3. [O III] λ5007 line profiles from OSU and Crimean data sets averaged over the same time span (JD 2448818–2448892). The profiles are normalized to the total flux of [O III] λ 5007 of $5.58 \cdot 10^{-13}$ergs cm^{-2} s^{-1}. It can be seen that the Crimean instrumental profile has more extended wings.

On the other side there are changes of the spectral resolution due to different observing conditions (even at the same instrumental settings). So, the adjustment of spectral resolution is needed, because changes of resolution will change the wing to core ratio. To remove this effect, we have estimated how much the resolution of each spectrum differs from the best resolution spectrum (the FWHM of the narrow lines was a criterion to select such a spectrum). It was done by convolution of the best resolution spectrum with the Gaussian function, optimizing its width by finding the maximally smooth residual at the [O III] line region between a given spectrum and convolved one. This procedure also includes the best centering of spectra on the wavelength scale. Then the resolution can be adjusted easily, assuming the instrumental profile is close to Gaussian. Note that only the resolution difference $\Delta\sigma_i$ was calculated. The resolution of a given spectrum in the assumption of a Gaussian-shaped instrumental profile is $\sigma_i = \sqrt{\sigma_0^2 + \Delta\sigma_i^2}$, where σ_0 is the best resolution. Thus, selecting the upper limit of resolution difference $\Delta\sigma_{max}$ we can exclude the spectra with lower resolution and adjust others to a given limit by convolution of i-th spectrum with a Gaussian profile with width $\sqrt{\Delta\sigma_{max}^2 - \Delta\sigma_i^2}$. After this

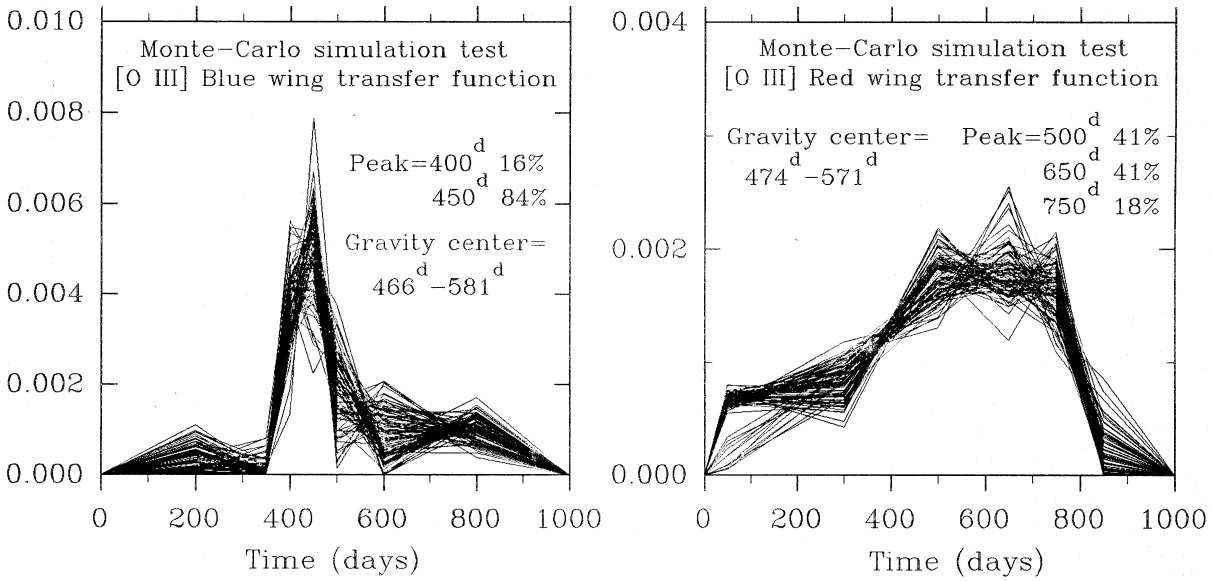

Fig. 4. The results of the Monte-Carlo test. The best fit curves from Fig. 2b,c were artificially noised and the transfer functions were reconstructed. The total of 100 loops have been done.

adjustment, our spectral collection has been reduced finally to 100 OSU and 87 Crimean spectra by dropping off total of 24 spectra with too low resolution including several spectra with too poor signal-to-noise ratio.

The wing fluxes were measured by direct integration of a spectrum at 5066–5078Å (observer frame) for the blue wing and 5104–5116Å for the red. The flux for the central part of the [O III] line was obtained at 5086.7–5094.7Å. The zones selected for the wings correspond to radial velocities of about ±1100 km s^{-1} relative to the line center. The continuum was fit by a straight line through the zones 4806–4840Å and 5160–5220Å.

The measurements based on the Crimean Observatory data set cannot be homogeneous with the OSU data set because the instrumental profile shapes differ. This leads to a systematic difference in the light curves between the two data sets due to the different amount of emission which is pumped from the narrow [O III] line to its wings. It can be illustrated by the example of [O III] λ5007 line profiles from the OSU and Crimean spectra (Fig. 3). While the non-variable flux of [O III] λ 5007 line for the selected zones must differ between data sets, the variable component must be approximately the same, since it is much wider than the instrumental profile. Therefore, the OSU and Crimean light curves for each selected zone will differ by a constant value. These constants were determined empirically by comparing pairs of nearly simultaneous observations (17 pairs separated by less than 7 days) from OSU and Crimean data sets.

The formal uncertainties of wing to core ratios due to the intercalibration procedure are ±0.0015 and ±0.0019 for the blue and red wings respectively. The wing to core ratios are shown in Fig. 2b,c. The error bars were calculated from the noise estimations in original spectra. Obtained error values are statistically consistent with point-to-point scattering of ±0.004 for both wing to core ratios. The variations are clearly pronounced, with an amplitude many times greater than the variations of the total [O III] line flux. We have applied the deconvolution method described in Sect. 3.1 to these data. The obtained transfer functions for the blue and red wings are shown in Fig. 2b,c (left panels). The transfer function for the blue wing is narrow-peaked near 450 days with no response up to 350 days lag. The red wing transfer function is wider with the peak at 650 days. The response near the zero lag is small but still present. To understand how significant these features are we have performed a Monte-Carlo test. Applying the deconvolution method to the artificially noised best fit and doing 100 loops, we have obtained a set of transfer functions which are shown in Fig. 4. As can be seen from this figure, all of the features mentioned above, including a peak displacement between the blue and red wing transfer functions, are significant. The sharper and shorter lag response for the blue wing may indicate the presence of outflow. However, the large span of no response for the blue wing while the red wing response is definitely present for the same span, as well as the fact that there is no significant difference between the transfer function centroids (see Fig. 4) cannot be explained by pure radial motion. We must conclude that the obtained transfer functions indicate complex kinematics, with no pure radial or round motions. The poor response near the zero lag must indicate the lack of emitting material near the line of sight, or that the material emits anisotropically. However, these suggestions have no sense in the case of the broad wings of the [O III] λ 5007 line being a blend of [O III] itself and Fe II λ 5018.

3.4. Changes in Fe II λ 5169

In order to compare the [O III] line variability with the variability of the numerous Fe II multiplets, we have studied changes of Fe II λ 5169 (m42). We chose this line because it is located

close to the continuum zone near 5100Å (5190Å for observer frame) which is relatively free from lines and thus the most suitable to measure the continuum under Fe II. This band was used to measure continuum flux in all AGN Watch observational papers (Peterson et al. 1991; Peterson et al. 1992; Peterson et al. 1994; Korista et al. 1995). We have selected the bands 5186–5196Å and 5487–5499Å (observer frame) to fit the continuum by a straight line and a zone 5245–5260Å (observer frame) to measure Fe II λ 5169 flux by direct integration. Unfortunately there is no suitable band to fit the continuum redward Fe II λ 5169. The band 5487–5499Å (observer frame) is within the strong Fe II blend of multiplets 48 and 49 which should vary as well as m42. However, these lines belong to the same ion Fe II and therefore must all vary in phase. Thus, the contribution of m48 and m49 lines to the continuum will only reduce the variation amplitude of Fe II λ 5169 line while will not affect its light curve by any other way. Note also that the more reliable blueward continuum zone at 5100Å (rest frame) is much closer to Fe II λ 5169. Several spectra do not cover the band 5487–5499Å and were omitted, so the total number of Fe II λ 5169 measurements is 158. From the obtained line light curve (Fig. 2d) we have reconstructed a transfer function (Fig. 2d, left panel) using the continuum light curve shown in Fig. 2e. The reconstructed transfer function is similar to that which has been obtained for the [O III] λ 5007 red wing. There is no response up to 150 days and there is a flat maximum near 500–600 days. The similarity may indicate that the broad wings of the [O III] λ 5007 line are dominated by the Fe II λ 5018 or that the [O III] broad emission feature originates at the same distance from the central engine as Fe II.

3.5. Decomposition of spectra into the short and long lag components

The observational evidences described above show that the optical spectrum of NGC 5548 contains emission features which vary with a large lag of hundreds of days relative to the optical continuum variations. To separate these features we must decompose the observed spectra into three components, namely the short lag component like that of broad Hβ, He II λ 4686 lines and non-stellar continuum, the slowly variable, long lag lines like of Fe II λ 5169 or [O III] λ 5007 wings, and the last component is the non-variable species which includes the narrow lines and stellar continuum. The decomposition scheme was described by Sergeev et al. (1994). Our approach is based on the variability characteristics. Let a spectrum contains several components, one of which is constant. Let also each of the variable components vary in flux, but not in the mean shape of its profile. For the simplest case of one variable and one non-variable component we can write:

$$L_{\lambda,t} = a_\lambda A_t + c_\lambda C \tag{3}$$

where C is the (unknown) integrated flux in the constant component, and a_λ, c_λ are the (unknown) normalized profiles of one variable and one non-variable component. The light curve of the variable component (A_t) can be written as the observed total flux minus constant flux: $A_t = L_t - C$, where $L_t = \int\limits_\lambda L_{\lambda,t} d\lambda$ is the total flux at the time moment t. There is a single solution of (3) for the profile shape of the variable component which can be found by the least-squares method:

$$a_\lambda \sim \frac{\sum\limits_t L_t L_{\lambda,t}}{\sum\limits_t L_t} - \frac{1}{n}\sum_t L_{\lambda,t} \tag{4}$$

(this is the same as the mean spectrum averaged with the weights equal to L_t minus the mean spectrum averaged with equal weights).

For a more complicated case of two variable ("A" and "B") and one constant component ("C") we have:

$$L_{\lambda,t} = a_\lambda A_t + b_\lambda B_t + c_\lambda C, \quad B_t = L_t - A_t - C \tag{5}$$

Now, there are an infinite number of solutions. However, if the light curve of one of the components is known, it gives us the profile shape of another component. It is easy to understand, because when subtracting any two spectra with the same brightness of "A" component while the brightness of "B" is not the same, the residual will give the profile of "B". Since the light curves of the short and long lag components are different, it allows us to separate these components. Note that a linear transformation of A_t and/or B_t leads to the redefinition of $c_\lambda C$ which changes the profile shape of the constant component while terms a_λ and b_λ become non-normalized but their profile shapes remain the same. So, such a linear transformation can be used to find variable component profile shapes, while the constant component c_λ cannot be found unambiguously. The least-squares method gives us the solution of Eq. (5) if the component light curves A_t and B_t are known:

$$a_\lambda \sim \frac{\frac{\sum A_t L_{\lambda,t}}{\sum A_t} - \frac{\sum L_{\lambda,t}}{n}}{\frac{\sum A_t B_t}{\sum A_t} - \frac{\sum B_t}{n}} - \frac{\frac{\sum B_t L_{\lambda,t}}{\sum B_t} - \frac{\sum L_{\lambda,t}}{n}}{\frac{\sum B_t^2}{\sum B_t} - \frac{\sum B_t}{n}} \tag{6}$$

where the summing is over t. The solution for b_λ can be obtained by the replacement $A \leftrightarrow B$ and $a \leftrightarrow b$. However, there is one difficulty. The profile shape of each component (which we assumed constant) for the real case of AGNs may vary. It can take place due to the evolution of the BLR (Wanders 1995) or because the BLR consists of several components with variable flux ratio (Sergeev et al. 1994). Thus, it is impossible to obtain the pure decomposed profiles.

Let us the light curve of one component, namely the short lag component is Hβ light curve (Peterson et al. 1991; Peterson et al. 1992; Peterson et al. 1994; Korista et al. 1995) corrected for the [O III] λ 5007 line variability. Let us take another, the long lag component light curve is the averaged light curve of [O III] λ 5007 blue and red wings (Fig. 2b,c). Applying the solution (6) to our spectra we have obtained these components separately (Fig. 5). As can be seen from Fig. 5, the long lag component (middle panel) can be identified with Fe II multiplets, although it is contaminated by the broad Hβ and perhaps

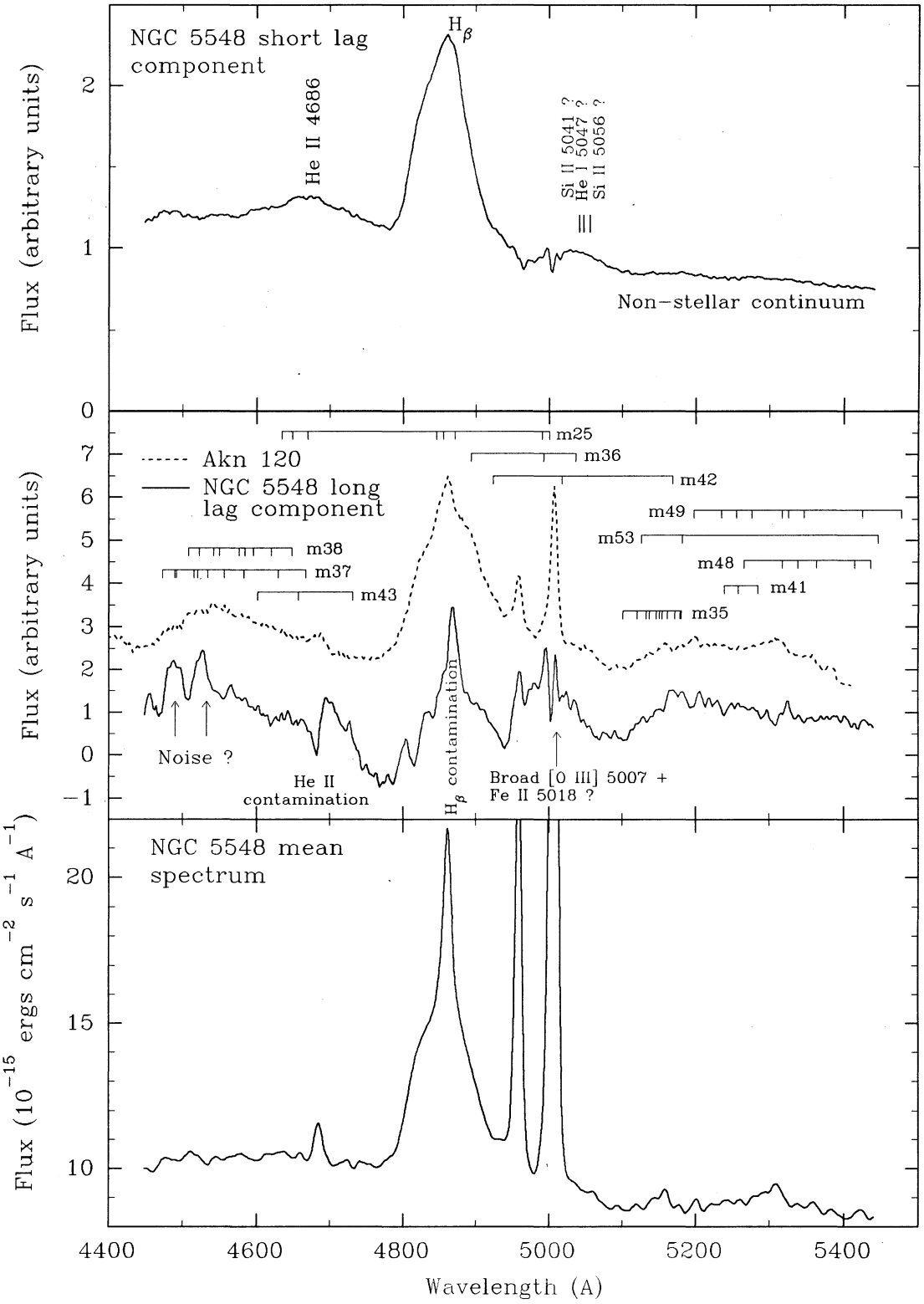

Fig. 5. NGC 5548 spectrum decomposition into the short and long lag components. The decomposition is based on the variability characteristics of all our spectra (see text, Eq. 6). The bottom panel spectrum is the average of all our spectra. The spectrum of the Fe II-rich object Akn 120 in the middle panel is shown to emphasize the position of Fe II multiplets and similarity with the long lag component of NGC 5548. The positions of Fe II multiplets observed in the spectra of Fe II-rich Seyfert galaxies as well as m25, m36, m53 are shown according to Phillips (1978) and Moore (1945).

He II λ 4686 lines. We have compared the long lag component with the spectrum of Akn 120 which is known as an Fe II-rich object and have found a large degree of similarity. The Akn 120 spectrum shown in the middle panel of Fig. 5 is the mean of four spectra obtained in the Crimean Observatory on JD 2449365, 9395, 9665 and 9713. So, by the decomposition procedure, we have enlarged the Fe II features making the spectrum of NGC 5548 very similar to the Fe II-rich spectrum of Akn 120. It was possible in the assumption that the long lag component has a light curve similar to that of [O III] λ 5007 wings. It allows us to make an important conclusion that all of the Fe II multiplets shown in Fig. 5 originate from a region with spatial extension of hundreds of days from the central engine, the same region as was obtained for [O III] wings. From the other side the Fe II multiplets are likely emitted in a high density region ($10^{10} \leq n_e \leq 10^{12}$ cm^{-3}) (Joly 1981, Joly 1987) where forbidden lines are collisionally deexcited. If so, we must attribute the [O III] λ5007 wings variations to Fe II lines, especially Fe II λ5018. Another possibility is the [O III] wings are emitted at similar distance from the central engine as Fe II but in low density gas.

The short lag component (Fig. 5 upper panel) consists of a non-stellar variable continuum and broad Hβ and He II λ 4686 species. One other line of the short lag component with gravity center of 5032Å may be identified with Si II λ 5041, 5056 (Crenshaw & Peterson 1986) or He I λ 5016, 5048. If so, the red wing of [O III] λ 5007 contains one additional fast-varying broad line. Note that this line is definitely present, because the emission at 5056 Å (rest frame) correlates with the optical continuum flux with a correlation coefficient of 0.514. Taking into account that the total number of measurements is 158, the probability of finding a correlation coefficient greater than 0.514 for a random sample is almost zero. From the other side, the emission at 5026Å where the red wing of [O III] λ 5007 was measured gives a correlation coefficient of 0.097. It proves that the long lag emission feature (Fe II λ 5018?) dominates here.

3.6. Conclusions

The analysis of [O III] λ 5007 wings and Fe II optical multiplet variability in NGC 5548 allows us to make the following conclusions:

1. The broad wings near the [O III] λ 5007 line are variable responding to the continuum variations with a typical lag of the order of several hundred days, while the narrow [O III] line, perhaps, does not vary. It suggests that these wings are emitted much farther from the central engine than the "usual" broad lines, maybe in the outer BLR.
2. As can be seen from the transfer functions of [O III] λ 5007 wings (Fig. 2b and c, left panels) there is a lack of emitting material near the line of sight. If the wings belong to a single broad line (e.g. Fe II λ 5018) we can conclude that there is no pure (symmetrical) radial or round motion, but the outflow component is definitely present.
3. The behavior of the Fe II λ 5169 line is similar to that of the [O III] λ 5007 wings (Fig. 2d). It proves that either Fe II λ 5018 is the main contributor to the [O III] wings or that the broad [O III] is emitted at the same distance from the central engine as Fe II.
4. The assumption about the presence of the short and long lag spectral components one of which varies similarly to the Hβ line and the other similarly to the [O III] λ 5007 wings permits us to separate these components (Fig. 5). The decomposition of the spectra shows that all observed Fe II multiplets (Fig. 5, middle panel) have a high lag value of the order of several hundred days. Thus the Fe II multiplets are emitted from the region of several hundred light days from the central engine.
5. The same decomposition shows that there is a short lag component in the red wing of the [O III] λ 5007 line (Fig. 5 upper panel). According to the gravity center of this line ($\approx$ 5032 Å) it may be identified with Si II λ 5041, 5056 or He I λ 5016, 5048.
6. The spectral calibration based on the assumption that the [O III] λ 5007 line is non-variable is not absolutely correct. For the case of NGC 5548 this line has varied by about 15% since 1977. For other objects and/or for other continuum behaviors these variations may be much larger. To improve data precision it is necessary to do absolute calibration using a comparison star or to account for the [O III] λ 5007 line variations if the transfer function is known.

Acknowledgements. This work was partially supported by the ESO C&EE grant A-01-057 and by the grant 2.3/737 of the Fundamental Research State Foundation of Ukraine. We are very grateful to Bradley Peterson and Ignaz Wanders (Ohio State University) for the valuable remarks and for the possibility to use their spectra of NGC 5548. We are also thankful to M. Joly for critical comments on the paper.

Appendix A: intercalibration of the "Pre-AGN Watch" data

In this appendix we will explain the intercalibration procedure of "Pre-AGN Watch" continuum measurements of NGC 5548. These measurements were compiled from the literature with codes for the origin shown in Table 1, where each data set is numbered consequently from 1 to 8. Now, we must recalculate these inhomogeneous data into the instrumental system of AGN Watch continuum measurements near 5100Å (Peterson et al. 1991; Peterson et al. 1992; Peterson et al. 1994; Korista et al. 1995, referred as AGN Watch papers).

The problems and methods of the intercalibration of AGN time-series are described in the AGN Watch papers. For the spectral data the corrections were done as follows:

$$F(cont) = \varphi F(cont)_{obs} - G. \quad \text{(A1)}$$

where a factor φ will account for the entrance aperture difference which leads to different amount of the light loss for the point source (broad lines and AGN continuum source) and extended NLR (narrow-line region). The extended source correction G is needed to adjust for the host galaxy contribution admitted by different apertures. The values φ and G were determined empirically by comparison of nearly simultaneous (to within two days)

observations from different data sets (see AGN Watch papers for more details). However, the "Pre-AGN Watch" time series taken from literature are based on the spectra which have been differently handled and measured by their authors. While it is quite impossible to account for the handling methods immediately it can be adopted at least that the different methods give the correlated (i.e. linearly related) results. Thus the Eq. A1 is still working, but now the φ and G must be redefined to reflect also the difference in the methods of the continuum measurements. The largest uncertainties must be due to the difference in the spectra scaling, while the term G seems to be more independent on methods. The Eq. A1 can be used also for both photometric data and measurements of equivalent widths of forbidden lines, but the stellar magnitudes must be converted into a linear scale, while the inverse equivalent widths must be taken.

The linear relationship between the light curves is a main point for the intercalibration, but for several cases we can also use the additional information. The stellar contribution through the nominal AGN Watch aperture ($5''.0 \times 7''.5$) is V_{gal} = 14.99 mag, or $F_\lambda(5100\,\text{Å}) = 3.4 \times 10^{-15}\,\text{ergs}\,\text{cm}^{-2}\,\text{s}^{-1}\,\text{Å}^{-1}$ (Korista et al. 1995). For the V-band measurements we also know the surface brightness distribution of the host galaxy (Romanishin et al. 1995). Thus we can calculate starlight contribution in this band for any aperture, convert it into the flux at 5100Å, subtract $3.4 \times 10^{-15}\,\text{ergs}\,\text{cm}^{-2}\,\text{s}^{-1}\,\text{Å}^{-1}$ and obtain the value of G (the case of data set 8). For those spectral data which were obtained with the same instrumental settings by the same people as in AGN Watch papers we can take at least the term G as determined in these papers (data sets 2,3,4,5).

In practice, the values φ and G were determined as regression coefficient and regression constant between the pairs of nearly simultaneous (separated up to three days) measurements from a given data set and AGN Watch continuum light curve merged with already homogenized data. If the term G is already known (several cases mentioned above), the value of φ is determined by direct division (see Eq. A1) of the nearly simultaneous measurements. We have started with largest and having many coinciding points data sets and gradually built up a large homogenized data base by adding smaller sets.

The following comments concern the individual data sets:

1. The data set 7 was calibrated at the beginning because it has a lot of nearly simultaneous measurements with the International AGN Watch data, permitting us to find a linear regression between these data sets. By the same way we have calibrated the data sets 1,6.
2. The data set 8 is the V-band photometry with round entrance aperture R=$7''.4$. It was calibrated as described above for the V-measurements with no particular comments.
3. The entrance slit width of data sets 2,3,4,5 was the same as in the International AGN Watch program. Thus G is known and only φ was calculated. For the data set 3, the value $2.3 \cdot 10^{-15}$ subtracted from the data by authors (Peterson et al. 1990) was added again. For the data set 2 the light curves at 4710–4760Å and 5375–5575Å were averaged to be closer to 5100Å. The data sets 5 and especially 4 require to relax the simultaneity criterion up to 5 and 14 days respectively.

References

Blandford, R. D., McKee, C. F. 1982, ApJ 255, 419
Chuvaev, K. K. 1987, IAU Symp. No 121, 203
Crenshaw, D. M., Peterson, B. M. 1986, PASP 98, 185
van Groningen, E. 1984, Ph.D. thesis, Sterrewacht Leiden
van Groningen, E., de Bruyn, A. G. 1989, A&A 211, 293
Joly, M. 1981, A&A 102, 321
Joly, M. 1987, A&A 184, 33
Korista, K. T. et al. 1995, ApJS 97, 285
Lyuty, V. M., Doroshenko, V. T. 1993, Pisma v Astron. Zh. 19, 995
Meyers, K. A., Peterson, B. M. 1985, PASP 97, 734
Moore, C. E. 1945, A Multiplet Table of Astrophysical Interest, Revised Ed. (Princeton, N.J.: Princeton University Observatory)
Netzer, H., Maoz, D., Laor, A., Mendelson, H., Brosch, N., Leibowitz, E., Almoznino, E., Beck, S., Mazeh, T. 1990, ApJ 353, 108
Osterbrock, D. E., Shuder, J. M. 1982, ApJS 49, 149
Peterson, B. M. 1994, in Reverberation Mapping of the Broad-Line Region in Active Galactic Nuclei, eds. Gondhalekar P. M., Horne K., Peterson B. M., ASP Conference Series 69, 1
Peterson, B. M., Korista, K. T., Cota, S. A. 1987, ApJ 312, L1
Peterson, B. M., Reichert, G. A., Korista, K. T., Wagner, R. M. 1990, ApJ 352, 68
Peterson, B. M. et al. 1991, ApJ 368, 119
Peterson, B. M. et al. 1992, ApJ 392, 470
Peterson, B. M. et al. 1994, ApJ 425, 622
Phillips, I. 1978, ApJS 38, 187
Rakhimov, V. Yu. 1989, Byull. Inst. Astrofiz. AN Tadz. SSR No 78, 50
de Robertis, M. 1985, ApJ 289, 67
Romanishin, W. et al. 1995, ApJ 455, 516
Sergeev, S. G., Malkov, Yu. F., Chuvaev, K. K., Pronik, V. I. 1994, in Reverberation Mapping of the Broad-Line Region in Active Galactic Nuclei, eds. Gondhalekar P. M., Horne K., Peterson B. M., ASP Conference Series 69, 199
Stirpe, G. M., de Bruyn, A. G. 1991, A&A 245, 355
Stirpe, G. M., de Bruyn, A. G., van Groningen, E. 1988, A&A 200, 9
Stirpe, G. M., van Groningen, E., de Bruyn A. G. 1989, A&A 211, 310
Wampler, E. J., Oke, J. B. 1967, ApJ 148, 695
Wanders, I. 1995, A&A 296, 332

This article was processed by the author using Springer-Verlag LaTeX A&A style file *L-AA* version 3.